available at www.sciencedirect.com

ScienceDirect

www.elsevier.com/locate/scitotenv

The use of a modelling system as a tool for air quality management: Annual high-resolution simulations and evaluation

Pedro Jiménez-Guerrero[a,], Oriol Jorba[a], José M. Baldasano[a,b], Santiago Gassó[b]*

[a]Earth Sciences Department, Barcelona Supercomputing Center-Centro Nacional de Supercomputación (BSC-CNS). Jordi Girona 29, Edificio Nexus II, 08034 Barcelona, Spain
[b]Environmental Modelling Laboratory, Technical University of Catalonia (LMA-UPC). Avda. Diagonal 647, Edificio H, Of. 10.25, 08028 Barcelona, Spain

ARTICLE INFO

ABSTRACT

The high levels of air pollutants over the North-Western Mediterranean (NWM) exceed the thresholds set in current air quality regulations. They demand a detailed diagnosis of those areas where the exceedances of thresholds related to human health are found. In this sense, there is a need for modelling studies for the specific area of the NWM that take into account the annual cycle to address the diagnosis of air pollution. A new approach to the modelling of air quality in the NWM has been adopted by combining the WRF-EMICAT-CMAQ-DREAM modelling system to diagnose the current status of the levels of photochemical air pollution (focusing on ozone, O_3; nitrogen dioxide, NO_2; carbon monoxide, CO; and particulate matter, PM10) in the area during an annual cycle (year 2004). The complexity of the area of study requires the application of high spatial and temporal resolution (2 km and 1 h). The annual simulations need to cover the complex different meteorological situations and types of episodes of air pollution in the area of study. The outputs of the modelling system are evaluated against observations from 52 meteorological and 59 air quality stations belonging to the Environmental Department of the Catalonia Government (Spain), which involve a dense and accurate spatial distribution of stations in the territory (32,215 km^2). The results indicate a good behaviour of the model in both coastal and inland areas of the NWM, with a slight trend to the overestimation of tropospheric O_3 concentrations and the underestimation of other photochemical pollutants (NO_2, CO and PM10). The modelling diagnosis indicates that the main air quality-related problems in the NWM are the exceedances of the 1-hr O_3 information threshold set in the Directive 2002/3/EC (180 μg m^{-3}) as a consequence of the transport of O_3 precursors downwind the Barcelona Greater Area (BGA); and the exceedances of the annual value for the protection of human health for NO_2 and PM10 (40 μg m^{-3}, Directive 1999/30/EC), both in the BGA, as a consequence of the high traffic-related emissions.

1. Introduction

The impact of air pollution, especially by ozone and particulate matter, is a key subject in climate and the environment (Akimoto, 2003; Baldasano et al., 2003). According to a study of the European Environmental Agency (EEA, 2005), air pollution is the environmental factor with the greatest impact on health in Europe and is responsible for the largest burden of

environment-related diseases. Particulate matter and especially small particles with a diameter less than 2.5 μm (PM2.5) are associated with increased mortality, especially from cardiovascular and cardiopulmonary diseases. The societal cost of asthma has been estimated at 3 billion euros per year.

In Europe, the mother Directive 1996/62/EC on air quality establishes the basic principia of a European common strategy to set the air quality objectives to avoid; prevent or reduce the harmful effects on the health and the environment. One of the topics in which the European Commission has shown a greater concern through initiatives as GMES (Global Monitoring for Environment and Security) is the necessity of developing actions that allow increasing the knowledge on transport and dynamics of pollutants to assure the accomplishment of legislation and to inform the population about the levels of pollutants, especially before 2010, date when directives 1999/30/EC and 2002/3/EC come into effect. The regulation is especially demanding when the threshold levels are exceeded. In this case, it demands a detailed diagnosis of those areas where the exceedances are found. Namely, the directive establishes the possibility of using modelling techniques to assess air quality.

A number of studies (e.g. Ziomas et al., 1998; Sanz and Millán, 1998; Sanz et al., 2000; Dueñas et al., 2002; Ribas and Peñuelas, 2004; Palacios et al., 2002, 2004) shows that the north-western Mediterranean Basin (NWM) frequently exceeds the thresholds of air quality established in the legislation. Additionally, not only the anthropogenic pollution contributes decisively to the failure in the meeting of European directives. Thus, the atmospheric mineral dust coming from deserts all around the planet represents an essential contribution to the content of tropospheric aerosols. The Sahara reveals as one of the most important dust sources, being northern Africa responsible for half of the global emissions of mineral dust. In the Iberian Peninsula, the mineral fraction of suspended particles comes from the local re-suspension and external contributions such as the Saharan/Sahelian dust (Pérez et al., 2006a,b), contributing to the exceedances of the PM10 limit values of Directive 1999/30/EC (Artíñano et al., 2001; Rodríguez et al., 2001; Rodríguez et al., 2002; Querol et al., 2004).

Under this perspective, air quality modelling is a useful tool for managing and assessing photochemical pollution that has been extensively used worldwide (e.g. Streit and Guzmán, 1996; Reis et al., 2000; Vinuesa et al., 2003). Historically, the models used for air quality assessment involved simplified Gaussian approaches or simply box models. The use of Eulerian models, which include a more realistic description of the atmosphere (especially in urban areas), has become more frequent during the last years (Seinfeld, 1988; Russell and Dennis, 2000). This work presents an assessment of the situation related with air quality for the year 2004 through high-resolution air quality modelling, focusing in the NWM. For that purpose, we have developed, implemented and validated an integrated air quality modelling system with a high resolution (2 km for the NWM), formed by a set of models that take into account both anthropogenic and natural pollution. The modelling system used for air quality simulations is WRF (meteorology)/EMICAT (emissions)/CMAQ (chemistry transport). The DREAM natural dust model (Nickovic et al., 2001) is finally used to estimate the mineral dust contribution. Despite the most important problems come from urban areas, the mesoscale models used through nested simulations have shown its efficacy when assessing air quality problems in cities, especially in areas with a complex topography as coastal regions (Fenger, 1999); in certain seasons, the urban areas can significantly affect and be affected by sources located hundreds of kilometres far from the point of study (Kallos, 1998). The models used represent the state-of-the-art in air quality modelling; they are highly supported and their behaviour is well-know for the NWM (e.g. Jiménez and Baldasano, 2004; Jiménez et al.; 2005a,b, 2006a,b).

2. Methods

The main objective is to assess the air quality in the NWM on an annual basis corresponding to the year 2004, focusing on the determination and diagnosis of the problems and exceedances related with tropospheric ozone (O_3), nitrogen dioxide (NO_2), carbon monoxide (CO) and particulate matter (PM10); as well as the evaluation of the results against air quality observations for the entire year 2004. Finally, an analysis of the obtained results with the simulations on an annual basis is compared with the thresholds established in the European regulations, assessing then the current status of air quality problems in the NWM.

The domains of study defined for the simulations are: Europe (D1, horizontal resolution of 54 km); the Iberian Peninsula (D2, 18 km); the north-eastern Iberian Peninsula (D3, 6 km) and NWM (D4, 2 km), despite the study focuses on D4. The domain covers 272 km × 272 km². This high resolution for this domain is needed because of the complexity of the area of study in order to describe the transport and transformation of pollutants, as well as the dynamics on an hourly basis (Jiménez et al., 2005a, 2006b). The relationship among the different domains simulated can be found in the Fig. 1. The Weather Research and Forecasting (WRF) Model (Michalakes et al., 2005; Skamarock et al., 2005) provides the meteorology dynamical parameters as inputs to CMAQ. The WRF model represents a next-generation mesoscale numerical weather prediction system designed for operational forecasting needs. WRF dynamical and physical options used for the simulations are: ARW dynamical core; Yonsei University PBL scheme; Kain-Fritsch cumulus scheme; single-moment 3-class microphysics' scheme; RRTM for long-wave radiation scheme and Dudhia scheme for short-wave scheme; and the Noah Land Surface Model. Initialization and boundary conditions for the mesoscale model are introduced with forecast data of the Global Forecast System of the National Center for Environmental Prediction (NCEP). Data are available at a 0.5-degree resolution (50-km approx. at the working latitude) at the standard pressure levels every 6 h. 366 simulations of 36 h have been performed (from 12 UTC of the previous day to the 00 UTC of the following day, with the aim of performing a cold initialization with 12 h of spin-up).

The high resolution (1 h and 1 km²) EMICAT emission model (Parra et al., 2006) has been applied to the domain. This model includes the emissions from vegetation, road-traffic, industries and emissions by fossil fuel consumption, domestic/
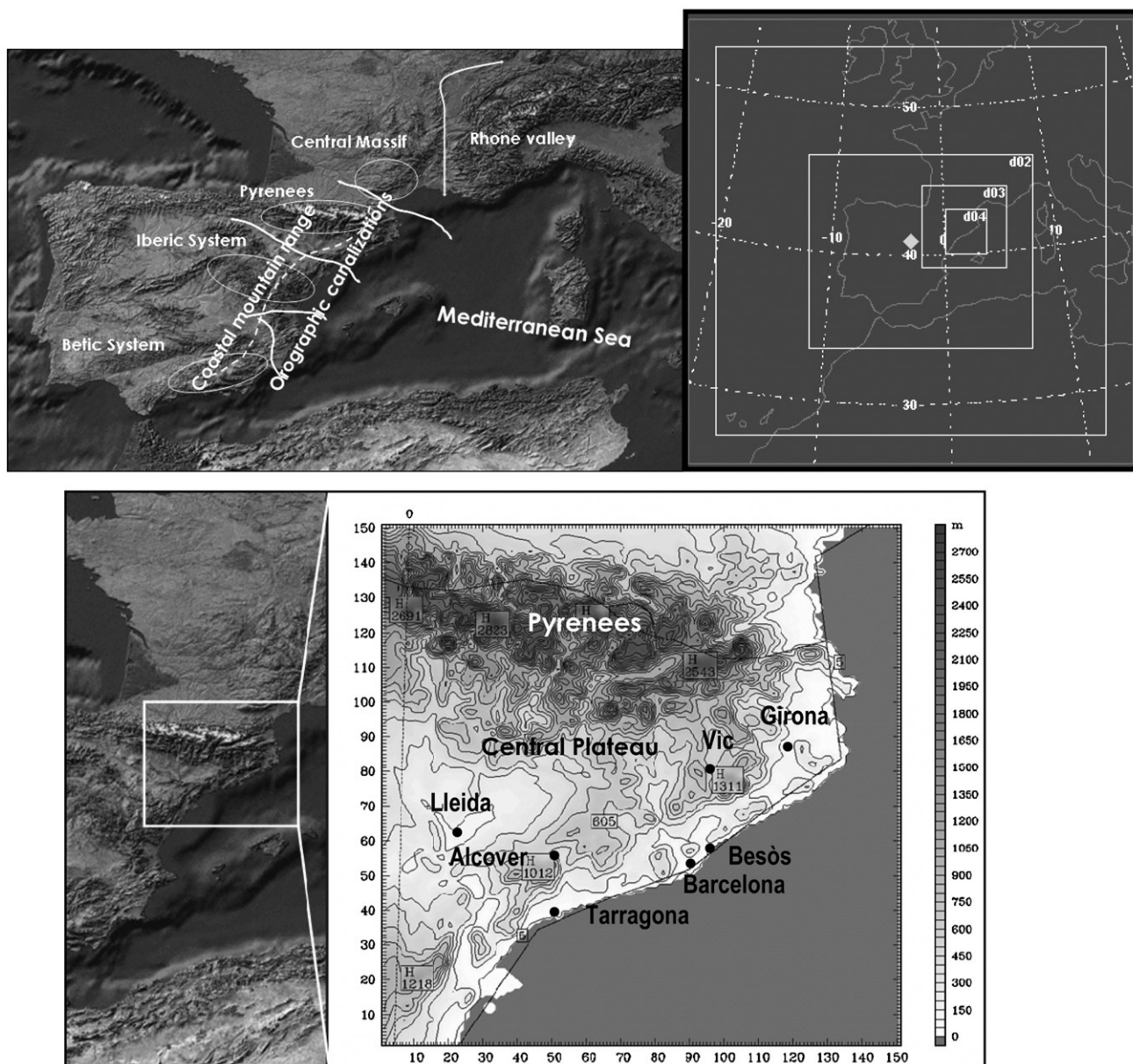
Fig. 1 – The north-western Mediterranean (NWM, top-left) nested domains (top-right) and topographical features in the area of study (bottom).

commercial and solvent use. Biogenic emissions were estimated using a methodology (Gómez and Baldasano, 1999) that takes into account local vegetation data (land-use distribution and biomass factors) and meteorological conditions (surface air temperature and solar radiation) together with emission factors for the native Mediterranean vegetation. Information derived from CORINE Land Cover Map of high resolution (100 m) was also used. Road traffic sources include the hot exhaust, cold exhaust and evaporative emissions using the methodology and emission factors of the European model EMEP/CORINAIR–COPERTIII (Ntziachristos and Samaras, 2000) as a basis, and distinguishing between the weekdays and weekends vehicle park composition (Jiménez et al., 2005b). Industrial emissions include records of some chimneys connected to the emission control net (XEAC) of the Environ-

mental Department of the Catalonia Government (Spain), and the estimated emissions from power stations (conventional and cogeneration units), cement factories, refineries, olefins plants, chemical industries and waste incinerators.

The main emission sources in the domain of study (Parra et al., 2006) (Table 1) are located on the coast, especially in the Barcelona urban area and the Tarragona industrial zone. Biogenic sources are also of great importance near the Mediterranean coast, representing 34% of the total annual non-methane volatile organic compounds (NMVOCs) emissions, especially since they contribute with reactive compounds such as aldehydes and isoprene. These emissions are particularly important during summertime because of the higher temperatures and solar radiation. The traffic emissions represent 58% of the emissions of NO_x and 36% of the

Table 1 – Summary of emissions by sources in the NWM as included in EMICAT (adapted from Parra et al., 2006)								
Source	Primary air pollutants (kt yr^{-1})						Greenhouse gases	
	NO$_x$	NMVOC	CO	SO$_2$	TSP	Total (a)	(kt CO$_2$ eq yr^{-1} (b)	(a)/(b)%
1. Vegetation		46.9				46.9		
2. On-road traffic	62.4	49.5	259.0	1.3	15.7	387.9	8302.0	4.7
3. Industrial emissions	41.2	22.8	7.3	61.1	7.5	139.9	20361.0	0.7
Power generation	15.0	0.7	2.1	28.5	1.7	48.0	5698.0	0.8
Cement	9.6	0.3	3.5	1.4	4.2	19.0	8477.0	0.2
Oil refineries	8.5	6.4	1.1	25.0	0.9	41.9	2929.0	1.4
Olefins	2.9	2.4	0.0	6.2	0.7	12.2	690.0	1.8
Fugitives emissions		11.0				11.0		
Other	5.2	2.0	0.6	0.0	0.0	7.8	2567.0	0.3
4. Fossil fuels use residential and commercial	3.3	0.2	1.1	2.3	0.3	7.2	3512.0	0.2
5. Use of solvents		17.2				17.2		
Total	106.9	136.6	267.4	64.7	23.5	599.1	32175.0	1.9
%	17.84	22.80	44.64	10.80	3.92	100		
Source	Primary air pollutants (kt yr^{-1})						Greenhouse gases	
	NO$_x$	NMVOC	CO	SO$_2$	TSP	Total	%	
1. Vegetation		34.33				7.83		
2. On-road traffic	58.37	36.24	96.86	2.01	66.81	64.75	25.80	
3. Industrial emissions	38.54	16.69	2.73	94.44	31.91	23.35	63.28	
Power generation	14.03	0.51	0.79	44.05	7.23	8.01	17.71	
Cement	8.98	0.22	1.31	2.16	17.87	3.17	26.35	
Oil refineries	7.95	4.69	0.41	38.64	3.83	6.99	9.10	
Olefins	2.71	1.76	0.00	9.58	2.98	2.04	2.14	
Fugitives emissions		8.05				1.84		
Other	4.86	1.46	0.22	0.00	0.00	1.30	7.98	
4. Fossil fuels use residential and commercial	3.09	0.15	0.41	3.55	1.28	1.20	10.92	
5. Use of solvents		12.59				2.87		
Total	100	100	100	100	100	100	100	

NMVOCs, notably olefins and aromatic compounds. During summer, especially in August, the traffic emissions increase with the growing number of tourist vehicles during the peak holiday period. Main sources are located at the axis of roads parallel to the coast and in the regions of Barcelona and Tarragona.

Industrial emissions represent 39% of the NO$_x$ and 17% of the NMVOCs emissions, and are located mainly in the industrial area of Tarragona. Further, the use of solvents represents 13% of NMVOCs emissions in the area. The source of precursors attributable to the industrial sector in the domain of study adds up to 41 kt yr^{-1} of NO$_x$ and 23 kt yr^{-1} of NMVOCs. Annually, total emissions of O$_3$ precursors include 106.9 kt yr^{-1} of NO$_x$ (58% traffic emissions; 39% industrial emissions) and 99.3 kt yr^{-1} of NMVOCs (34% biogenic emissions; 36% road traffic; 17% industrial emissions). The ratio NMVOCs/NO$_x$ is 1.28 on the annual average, increases up to 1.73 for summertime due to the high temperatures and solar radiation, promoting e.g. evaporative emissions from vehicles, storage of fuels and solvents, and by the vegetation.

The chemistry transport model used to compute the concentrations of photochemical pollutants in the domain of the Iberian Peninsula (D2) and NWM (D4) was Models-3/CMAQ (Byun and Ching, 1999). The initial and boundary conditions for D4 were derived from a one-way nested simulation covering a domain of 1392×1104 km^2 centred in the Iberian Peninsula with a resolution of 18 km (D2), that used EMEP emissions corresponding to year 2004. The boundary condi-

tions of the mother domain (D2) were derived from climatologic profiles of atmospheric pollutants as described in Byun and Ching (1999). The inner domain (D4) covers an area of 272×272 km^2 with a high horizontal resolution of 2 km. A 48-hour spin-up was performed to minimise the effects of initial conditions for both domains. The chemical mechanism selected for the simulations (following the criteria of Jiménez et al., 2003) was CBM-IV (Gery et al., 1989), including aerosols and heterogeneous chemistry. The algorithm chosen for the resolution of the tropospheric chemistry was the Euler Backward Iterative (EBI) method. With respect to dry deposition, the M3DDEP module (Pleim et al., 1996) has been used in the simulations. A further description of the model setup could be found in Jiménez and Baldasano (2004). The horizontal resolution considered was 2 km, and 16-sigma vertical layers cover the lower troposphere.

Last, the model used to provide the concentrations of desert dust is the Dust REgional Atmospheric Model (DREAM) (Nickovic et al., 2001). The dust concentrations are added to the anthropogenic PM10 concentrations estimated with CMAQ. This addition is performed by using a bi-linear interpolation of CMAQ and DREAM integration grids into a unique common grid with CMAQ's resolution. DREAM is fully inserted as one of the governing equations in the atmospheric NCEP/Eta atmospheric model and simulates all major processes of the atmospheric dust cycle. Wind erosion of the soil is parameterized by the type of soil, vegetation cover, soil moisture content, and surface atmospheric turbulence. In the

operational version, for each texture class fraction four particle size classes (clay, small silt, large silt and sand) are estimated with particle size radii of 0.73, 6.1, 18 and 38 μm, respectively. DREAM is extensively used and validated by the scientific community (e.g. Ansmann et al., 2003; Pérez et al., 2006a,b; Balis et al., 2006; Papayannis et al., 2007).

The resolution applied requires of a great capacity of super-computation. The availability of the MareNostrum supercomputer hold in the Barcelona Supercomputing Center-Centro Nacional de Supercomputación (BSC-CNS) together with the advances in the parallelization of air quality model codes for their implementation in these high performance computing infrastructures, have allowed high-resolution simulations on medium-and long-term simulations (e.g. the needed time for integrating annual air quality simulations in the NWM has reduced from 315.2 days with a single-processor machine to 2.7 days using 200 MareNostrum processors, as shown in Table 2).

3. Results and discussion

3.1. Meteorology: dynamics of the NWM and evaluation of modelling results

The Iberian Peninsula and the Western Mediterranean Basin are characterized by its complex topography and a particular

Table 2 – Computing time for the four meteorological domains in the MareNostrum supercomputer and comparison of time for D4 air quality integrations in a single-processor vs. MareNostrum supercomputer

Meteorological simulations, D1 to D4				
MareNostrum supercomputer, 94.21 teraflops of theoretical performance peak, 10240 processors PowerPC 970MP				
Domain (size)	Horizontal resolution (km)	Processors	Simulated h/h	Days for simulating 1-yr
D1 (55×55×32)	54	40	1087.0	0.3
D2 (94×82×32)	18	40	540.5	0.7
D3 (106×103×32)	6	120	270.3	1.4
D4 (154×169×32)	2	240	86.4	4.3
Air Quality Simulations, D4 (NWM), 2 km resolution				
HP Workstation XEON 3.3 GHz				
Processors	Time to simulate 1 day (s)	Time to simulate 1 day (min)	Simulated h/h	Days for simulating 1-yr
1	74419	1240.32	1.3	315.2
MareNostrum supercomputer, 94.21 teraflops of theoretical performance peak, 10240 processors PowerPC 970MP				
40	1741	29.01	49.6	7.4
70	1101	18.35	78.5	4.7
100	902	15.03	95.8	3.8
150	742	12.37	116.4	3.1
200	640	10.67	135.0	2.7

location between two continents, a major ocean and a small-warm sea. The cloud-free conditions and high solar radiation intensity promote the photochemical build-up of ozone and other pollutants (Lelieveld et al., 2002). These particularities and the global circulation at middle latitudes induce several different meteorological and a particular behaviour of the dynamics of air pollutants related to this atmospheric evolution. For the Western Mediterranean, the project ESCOMPTE (Cros et al., 2004) showed the high occurrence of photochemical pollution events in the area of southern France. These results highlighted the dynamical characteristics of the area. While the Iberian Peninsula becomes isolated from the travelling lows and their frontal systems in summer with high occurrence of stagnant situations, in winter the weather is characterized by an increase of extra-tropical cyclone activity. The complex topography of the area induces an extremely complicated structure of the flow because of the development of large and local mesoscale phenomena that interact with synoptic flows. Modelling results indicate that sea breeze circulation and channelling effects due to terrain features strongly influence the location of the pollutant plumes (Dufour et al., 2005; Kalthoff et al., 2005; Jiménez et al., 2006b). In addition, the flow can be even more complex because of the non-homogeneity of the terrain, the land-use and the types of vegetation. In these situations, the structure of the flow is extremely complicated because of the overlap of circulations of different scale.

The simulations results indicate that the NWM is characterized by a complex topography (Fig. 1) that shapes the surface wind flows with a marked decoupling of the lower from the middle troposphere. The analysis of the annual cycle simulation allows identifying the distinctive wind flow patterns developed within the domain of study and its relation with air quality. Winter situations are characterized by the development of local winds (Bougeault et al., 1990, 1997), as cierzo (north-western local wind developed in the Ebro Valley) or tramontana (northern wind locally developed in the north-eastern part of the NWM) through the major valley canalizations and an overwhelming of the synoptic flow over the region, while typical summertime situations are characterized by the development of thermal circulations (e.g., mountain winds, sea-breeze). This region is usually affected by moderate to strong north-western winds (e.g., cierzo) when western-north-western synoptic situations affect the Iberian Peninsula. On the other hand, during stagnant situations the Ebro valley is a typical region with low or calm winds and high temperatures. In the same way, the inland plateaus present a similar behaviour, with weak thermal flows during summer with an important development of the boundary layer and strong winds with enhanced subsidence during wintertime.

The Pyrenees represents the major orographic feature of the region, as one of the highest mountain ranges in Europe. The flows over the Pyrenees present a complex vertical structure, with the development of mountain waves and downslope warm and dry winds as the Föhen wind (e.g., Whitemann, 2000). The coastal zone presents also a distinctive wind flow pattern characterized by the sea-breeze flows during summer, and synoptic overwhelming flows during

winter. On-shore winds advect pollutants form the coastal high urbanized zones to the inland regions. The strength of the on-shore flows and the complex orography of the NWM coast may produce several injections due to orographic forcing. As the on-shore front advances inland reaching the mountain ranges, orographic injections occur at different altitudes (Jorba et al., 2003). A number of studies have shown that during summertime, layering and accumulation of pollutants such as ozone and aerosols were taking place along the eastern Iberian Peninsula (Millán et al., 1992, 1997; Pérez et al., 2004). These mechanisms together with the development of a low coastal boundary layer (Sicard et al., 2006) are mainly responsible of the high levels of air pollutants observed inland.

The results of the WRF meteorological model have been evaluated with observations from a set of 52 surface meteorological stations distributed in the NWM belonging to the Catalonia Meteorological Service, which involves a dense and accurate spatial distribution of stations in the territory. The evaluations include the speed and wind direction at 10 m, and air temperature at 2 m. The root mean square error (RMSE) and bias error for these parameters have been calculated from hourly data of the model and observations, obtaining a daily statistical value. Last, the wind speed statistics are only estimated for a wind speed threshold of 0.5 m s^{-1} in order not to have into account the calm situations. The equations applied for the statistical evaluation are indicated in Eqs. (1) and (2).

$$\text{RMSE} = \sqrt{\sum_{i=1}^{N} \frac{(\phi_i - \phi_{iobs})^2}{N}} \qquad (1)$$

$$\text{BIAS} = \sum_{i=1}^{N} \frac{(\phi_i - \phi_{iobs})}{N} \qquad (2)$$

where ϕ_i is the forecasted value for the cell i, ϕ_{iobs} is the value observed for the cell i, and N is the number of values analysed. Last, the wind direction is a cyclic variable, and then statistical parameters should be carefully considered. A feasible possibility is to use the root mean square vector error (RMSVE) to have an idea of the magnitude of the correctness of the vector. If the RMSE is used, then the difference between simulated and observed direction should be minimum in absolute value. So, the RMSE of the direction is estimated as (Eqs. (3) and (4)):

$$\text{RMSE}_{\text{dir}} = \sqrt{\sum_{i=1}^{N} \frac{D^2}{N}} \qquad (3)$$

$$D = \min(|d_i - d_{iobs}|, |360 + (d_i - d_{iobs})|) \qquad (4)$$

where d_i is the horizontal wind direction forecasted for the cell i, d_{iobs} is the horizontal wind direction observed for the cell i, and N is the number of analysed values. For the bias, a positive (negative) bias involves a tendency of the model to simulate wind vectors right (left) to the observations (Eq. (5)):

$$\text{BIAS}_{\text{dir}} = \sum_{i=1}^{N} \frac{D}{N}; \qquad (5)$$

if $d_i < d_{iobs}$:

$$D = d_i - d_{iobs} \text{ if } |d_i - d_{iobs}| < |360 + (d_i - d_{iobs})|$$

$$D = 360 + (d_i - d_{iobs}) \text{ if } |d_i - d_{iobs}| > |360 + (d_i - d_{iobs})|$$

if $d_i > d_{iobs}$:

$$D = d_i - d_{iobs} \text{ if } |d_i - d_{iobs}| < |(d_i - d_{iobs}) - 360|$$

$$D = (d_i - d_{iobs}) - 360 \text{ if } |d_i - d_{iobs}| > |(d_i - d_{iobs}) - 360|$$

The Fig. 2 shows the evolution of the RMSE and bias of the wind speed at 10 m, the wind direction at 10 m and the air temperature at 2 m. The wind speed at 10 m (Fig. 2a) depicts a RMSE delimited between 2 and 4 m s^{-1} during most of the year. The highest deviations are observed during wintertime, with RMSE over 5 m s^{-1}, reaching 8 m s^{-1}. The meteorological situations with a higher deviation from the average behaviour in the surface winds are characterized by the presence of the winter anticyclone over the Atlantic, west or north of the Iberian Peninsula, inducing northeast flows in the NWM. These situations are distinguished by the development and evolution of a low in the western Mediterranean. The model overestimates the strong flows in the NWM. The presence of the Pyrenees is considered as a key factor to understand the performance of the model in the area related to the downwind flows; the behaviour of the model is conditioned by the location of the boundaries of the inner domains and the resolution of the nested simulations.

During the central part of the year, the model performs with a RMSE lower than 4 m s^{-1}, being this error under 3 m s^{-1} in most of the period. This is characterized by meteorological situations with stagnant situations in the region, with the development of the Iberian Thermal Low and a dominance of breeze regimes in the coasts and mountains winds inland (Millán et al., 1992). Several authors have pointed that low air quality episodes develop in southern Europe associated to local-high formation rates of photochemical pollutants within these stagnant situations (Coll et al., 2005; Cousin et al., 2005; Dufour et al., 2005; Jiménez et al., 2006b). The model presents a fairly good behaviour when compared with observations, despite it tends to underestimate the breezes during the day and, at night, the model does not accurately reproduce the calms or the very weak winds typical of the region during summertime. This causes the positive bias observed in wind speed; the model overestimates the nocturnal surface winds, a phenomenology which is currently not fully resolved in meteorological models.

The Fig. 2b also presents the evolution of the RMSE and the bias of the wind direction at 10 m. The RMSE ranges between 60 and 90°. The months of April and November show the highest deviations; however the model presents a smooth and good behaviour during the rest of the year. There is a trend to simulate directions with positive bias periods. The evolution of the error in air temperature at 2 m is shown in the Fig. 2c. The RMSE of this temperature ranges between 2 and 4 °C during most of the year 2004. The highest errors are produced in two wintertime situations; meanwhile the rest of the year they remain around 3 °C. During summertime, the improvement in the evaluation results when increasing resolution (Fig. 2d) is
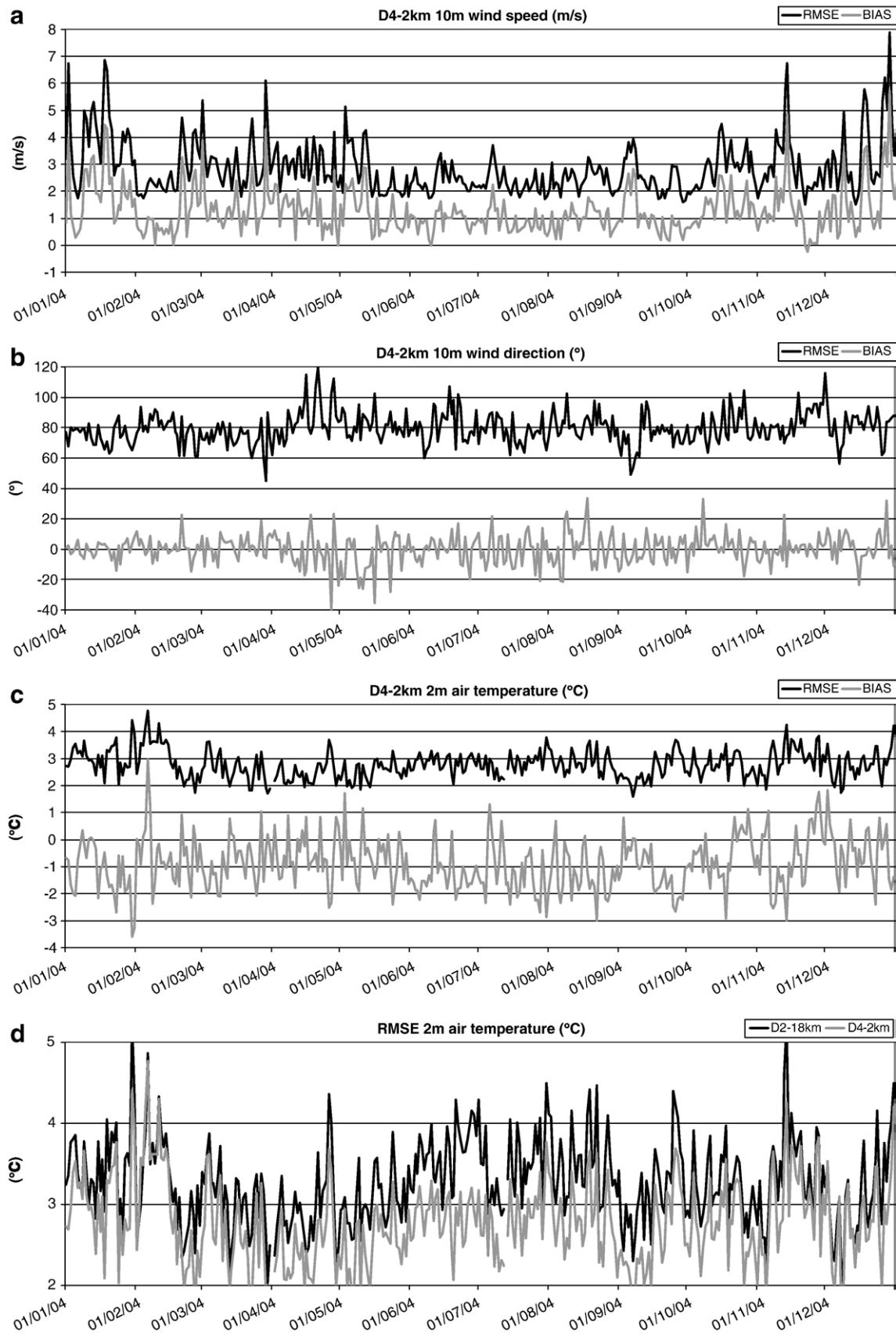
Fig. 2 – Annual evolution of the daily RMSE and BIAS error in the NWM for 2 km horizontal resolution simulations: (a) RMSE (black) and BIAS (grey) of 10-m wind speed; (b) RMSE (black) and BIAS (grey) of 10-m wind direction; (c) RMSE (black) and BIAS (grey) of 2-m air temperature; (d) RMSE of 2-m air temperature for the results of D2, Iberian Peninsula (18 km, black); and D4, NWM (2 km, grey).

more evident; so, the RMSE can be improved in more than 1 °C when comparing the results with different resolutions (2 km vs. 18 km). During wintertime the differences in the temperatures between the different resolutions are not obvious, because of the dominance of advective synoptic situations, meanwhile in summer the stagnant situations (mesoscale) are more important. The bias highlights the tendency to underestimate the temperature in low levels.

The performance of the meteorological model agrees with several previous works focused in meteorological applications for air quality modelling (Ulrickson and Mass, 1990; Seaman et al., 1995; Lyons et al., 1995; Fast, 1995; Shafran et al., 2000; Deng et al., 2004; Jiménez et al., 2006a), where the classical statistics for surface fields (e.g., temperature, wind speed) range from 1 to 4 °C and 2 to 4 m s^{-1} under different meteorological situations, in a wide agreement with the results presented in this work. The daily averaged statistics shown in the work reflects the main performance of the model, though more detailed hourly statistics depict a tendency to overestimate nocturnal flows and understimate the intensity during the day (not shown).

3.2.   Evaluation of the chemistry transport model

Air quality station hourly data, averaged over the domain of study were used to evaluate the performance of the modelling system for predicting ground-level O_3, NO_2, CO and PM10 during the year 2004. Measurements of ambient pollutants were reported by 59 air quality surface stations (XVPCA) in the NWM, which are part of the Environmental Department of the Catalonia Government (Spain). This network provides air quality data for urban, industrial and background areas with an accurate territorial distribution, and it represents one of the most dense air quality networks in Europe (since the 59 stations are distributed in an area of just 32,215 km^2). The European Directives 2002/3/EC and 1999/30/EC assume an uncertainty of 50–60% for the air quality objective for modelling assessment methods. This uncertainty is defined as the maximum error of the measured and calculated concentration levels. In addition, the US Environmental Protection Agency has recently developed new guidelines (US EPA, 2005) for a minimum set of statistical measures to be used for these evaluations in regions where monitoring data are sufficiently dense. These guidelines indicate that it is inappropriate to establish a rigid criterion for model acceptance or rejection (i.e., no pass/fail test). However, in the EPA guide for the 1-hour ozone attainment demonstrations (US EPA, 1991), several statistical goals were identified for operational model performance. These goals were identified by assessing past modelling applications of ozone models and determining common ranges of bias, error, and accuracy. These statistical measures considered are the mean bias (MB); the mean normalized bias error (MNBE); the mean normalized gross error for concentrations above a prescribed threshold (MNGE), and the unpaired peak prediction accuracy (UPA). The accepted criteria are: MNBE, ±5 to ±15%; MNGE, +30 to +35%; UPA ±15 to ±20%. The results presented below show the evaluation of the annual average values during the year 2004; however, the correlation coefficients measure the skill for daily means information. A summary of the used statistics is found in the Table 3.

Table 3 – Statistical figures used in the evaluation of atmospheric pollutants simulated by the air quality modelling system (Model: modelled data (obtained from simulations); Obs: observations (ambient data); N: number of observations)

Mean bias (MB)	$MB = \frac{1}{N}\sum_1^N (Model - Obs)$
Mean normalized bias error (MNBE)	$MNBE = \frac{1}{N}\sum_1^N \left(\frac{(Model - Obs)}{Obs}\right) \cdot 100\%$
Mean fractionalized bias (MFB)	$MFB = \frac{1}{N}\sum_1^N \left(\frac{(Model - Obs)}{\left(\frac{Model + Obs}{2}\right)}\right) \cdot 100\%$
Mean absolute gross error (MAGE)	$MAGE = \frac{1}{N}\sum_1^N |Model - Obs|$
Mean normalized gross error (MNGE)	$MNGE = \frac{1}{N}\sum_1^N \left(\frac{|Model - Obs|}{Obs}\right) \cdot 100\%$
Normalized mean error (NME)	$NME = \frac{\sum_1^N |Model - Obs|}{\sum_1^N Obs} \cdot 100\%$
Normalized mean bias (NMB)	$NMB = \frac{\sum_1^N (Model - Obs)}{\sum_1^N (Obs)} \cdot 100\%$
Root mean square error (RMSE)	$RMSE = \sqrt{\frac{1}{N}\sum_1^N (Model - Obs)^2}$
Unpaired peak accuracy (UPA)	$UPA = \frac{Model_{max} - Obs_{max}}{Obs_{max}} \cdot 100\%$

The Tables 4 and 5 and Fig. 3a indicate that the model presents a tendency to overestimate the ground-level ozone concentration in the different stations in the NWM (MB, 2.2 µg m^{-3}; MNGE, 21% and UPA, +11%). The correlation between observed and simulated values (Fig. 4) is $r = 0.848$, indicating a strong correlation. For the stations in the Barcelona Greater Area (BGA), the model underpredicts the measured values: MB, −4.5 µg m^{-3}; MNGE, 26%; and UPA, −17%. This increase in the errors for ozone assessment in urban downtown areas comes conditioned by the weaknesses of models to represent the nocturnal physico-chemical processes; and also by somewhat underestimated climatic background values through the boundaries of the domain of the Iberian Peninsula. However, the average results are within the regulatory framework recommended in the European Directive 2002/3/EC.

For the nitrogen dioxide, the concentration of this pollutant is accurately predicted in the stations of the NWM (MB, 1.9 µg m^{-3}; MNGE, 25%; UPA, −9%) (Tables 4 and 5 and Fig. 3b). The value of the correlation coefficient is significant ($r = 0.794$). For BGA, the MNGE value slightly improves, since the on-road traffic pervasive emissions and local photochemistry dominate in urban areas versus other contributions such as e.g. advective or convective transport; and also the influence of boundary conditions decrease (Jiménez et al., 2006b). The statistical values turn into: MB, 6.1 µg m^{-3}; MNGE, 24%; UPA, −9%. The underestimation in the peak values may be caused because a relatively coarse vertical resolution of the lower troposphere leads to artificial vertical exchange between the boundary layer

Table 4 – Annual average observed values vs. simulated concentrations of tropospheric ozone, nitrogen dioxide, carbon monoxide and particulate matter (anthropogenic and natural) in the NWM for the year 2004

Station	LON	LAT	O_3 ($\mu g\ m^{-3}$) Obs	Annual average 2004 Mod	NO_2 ($\mu g\ m^{-3}$) Obs	Annual average 2004 Mod	CO ($\mu g\ m^{-3}$) Obs	Annual average 2004 Mod	PM10 ($\mu g\ m^{-3}$) Obs	Annual average 2004 Mod
Agullana	2.843	42.393	71	79	–	–	–	–	–	–
Alcover	1.168	41.263	64	66	–	–	–	–	–	–
Amposta	0.583	40.708	52	47	–	–	–	–	–	–
Badalona	2.240	41.445	39	24	51	52	0.4	0.4	–	–
Barbera del Valles	2.127	41.514	–	–	28	41	0.5	0.3	54	37
Barcelona (Ciutadella)	2.189	41.388	29	28	43	58	0.5	0.5	–	–
Barcelona (Eixample)	2.155	41.386	34	26	60	61	0.9	0.7	55	52
Barcelona (Gracia St. Gervasi)	2.154	41.400	14	25	67	61	0.5	0.5	–	–
Barcelona (Poblenou)	2.205	41.405	33	28	40	58	0.5	0.5	–	–
Barcelona (Sagrera)	2.192	41.424	–	–	–	–			52	48
Barcelona (Sants)	2.134	41.380	–	–	36	52	0.5	0.5	–	–
Begur	3.214	41.960	72	69	–	–	–	–	–	–
Bellver de Cerdanya	1.778	42.369	60	75	11	9	–	–	–	–
Constanti	1.219	41.156	59	59	20	21	–	–	30	26
Cornella	2.078	41.358	–	–	39	48	–	–	–	–
El Prat de Llobregat	2.094	41.333	–	–	52	52	–	–	44	38
Gandesa	0.441	41.059	65	61	–	–	–	–	–	–
Gavà (C/Girona C/Progres)	2.015	41.302	29	29	–	–	–	–	–	–
Gavà (Parc del Milleni)	1.993	41.304	24	28	37	41	–	–	–	–
Gavà (Pl. Balmes)	2.001	41.305	–	–	22	39	–	–	–	–
Girona (Parc de la Devesa)	2.812	41.986	–	–	34	13	0.6	0.3	–	–
Granollers (Joan Vinyoli)	2.280	41.601	41	32	31	37	0.6	0.3	53	39
Igualada	1.627	41.579	32	44	26	22	0.5	0.3	38	24
Juneda	0.818	41.551	62	64	–	–	–	–	–	–
La Senia (Repetidor)	0.289	40.644	70	65	–	–	–	–	–	–
l'Hospitalet de Llobregat	2.116	41.372	35	21	36	52	0.5	0.5	34	35
Lleida	0.617	41.617	43	57	25	9	0.4	0.2	42	22
Manresa	1.826	41.731	27	33	32	19	0.6	0.4	–	–
Martorell	1.922	41.477	27	41	36	34	0.5	0.3	39	33
Montcada i Reixac	2.190	41.483	29	24	36	45	–	–	45	39
Montornes del Valles	2.268	41.554	–	–	–	–	–	–	39	37
Pardines	2.215	42.313	80	89	–	–	–	–	–	–
Perafort	1.238	41.195	–	–	12	19	–	–	–	–
Ponts	1.196	41.905	46	57	–	–	–	–	39	20
Reus	1.121	41.152	50	52	19	21	0.4	0.3	–	–
Rubi (Can Oriol)	2.044	41.493	40	37	23	32	0.4	0.3	39	33
Sabadell (Av. Gran Via)	2.103	41.562	28	30	43	41	0.7	0.4	47	39
Sabadell (Pl. Creu de Barbera)	2.119	41.530	–	–	–	–	–	–	37	35
Sant Adria de Besos	2.223	41.427	36	21	34	47	0.4	0.4	52	45
Sant Andreu de la Barca	1.976	41.452	27	26	44	33	–	–	46	41
Sant Celoni	2.497	41.690	32	31	31	28	–	–	41	25
Sant Cugat del Valles	2.090	41.478	31	41	32	44	0.5	0.5	39	37
Sant Fost	2.224	41.529	27	34	–	–	–	–	–	–
Sant Vicenç dels Horts	2.011	41.393	–	–	43	45	–	–	49	40
Sort	1.131	42.407	59	79	–	–	–	–	–	–
Sta. Coloma de Gr. (Balldovina)	2.210	41.448	30	35	48	49	0.3	0.3	–	–
Sta. Coloma de Gr. (C/Bruc)	2.218	41.452	46	35	–	–	–	–	26	28
Sta. Maria de Palautordera	2.443	41.692	52	46	–	–	–	–	–	–

Table 4 (*continued*)

Station	LON	LAT	O$_3$ ($\mu g\ m^{-3}$) Obs	Annual average 2004 Mod	NO$_2$ ($\mu g\ m^{-3}$) Obs	Annual average 2004 Mod	CO ($\mu g\ m^{-3}$) Obs	Annual average 2004 Mod	PM10 ($\mu g\ m^{-3}$) Obs	Annual average 2004 Mod
Sta. Perpetua de Mogoda	2.218	41.537	–	–	–	–	–	–	57	45
Tarragona (Bonavista)	1.193	41.117	51	51	23	21	0.5	0.3	35	28
Tarragona (Parc de la Ciutat)	1.243	41.119	–	–	28	21	–	–	31	28
Tarragona (Pl. Generalitat)	1.242	41.122	–	–					47	28
Tarragona (St. Salvador)	1.241	41.161	–	–	26	21	0.4	0.3	31	27
Tarragona (U. Laboral)	1.202	41.105	–	–	23	21	–	–	–	–
Tona	2.222	41.848	25	55	–	–	–	–	54	24
Vic (Hospital de la Santa Creu)	2.252	41.929	52	62	–	–	–	–	–	–
Vilanova i la Geltru	1.722	41.220	46	59	25	17	0.3	0.3	37	26
Vila-seca	1.153	41.113	54	55	20	21	–	–	37	24
Zona Port de Barcelona (Darsena Sud)	2.147	41.335	43	38	–	–	–	–	56	50

and the free troposphere, which enhances nitrogen oxides venting from the planetary boundary layer (Wang et al., 1998). The Fig. 3b depicts the best comparisons of the observed and simulated values in the BGA and the industrial area of Tarragona, in the southern coast of the domain, because of the better spatial representation in the estimation of emissions (Parra et al., 2006). On the other side, the most important deviations are observed in the inland cities of Girona and Lleida, where the urban on-road traffic emissions are not fully characterized. The statistical values meet the reference values for uncertainty air quality modelling set in the European Directive 1999/30/EC.

The most accurate results are found for carbon monoxide (Table 4 and 5 and Fig. 3c). In the NWM domain, the MB is −0.109 mg m^{-3}; MNGE, 21% and UPA, −11%. The correlation coefficient is $r=0.622$. For BGA, the performance of the model improves (MB, −0.009 mg m^{-3}; MNGE, 8%; UPA, −11%). As noted by Russell and Dennis (2000), current air quality models have a pervasive tendency towards the underprediction of ozone precursors (both nitrogen oxides, carbon monoxide and volatile organic compounds).

In the case of particulate matter PM10, the contribution of Saharan dust in the NWM has been taken into account, by using the year 2004 simulations of the Dust Regional Atmospheric

Model (DREAM) model that estimates the synoptic average annual concentrations around 4.9 μg m^{-3} in the domain of the NWM (http://www.bsc.es/projects/earthscience/DREAM/). The Tables 4 and 5 and Fig. 3d indicate that the model underestimates the annual average concentration observed in the NWM (MB, −8.2 μg m^{-3}; MNGE, 19%; UPA, −9%). The correlation coefficient is $r=0.669$. For the BGA, the primary anthropogenic particles increase and the statistical values improve (MB, −3.9 μg m^{-3}; MNGE, 10%; UPA, −7%). Especially for the BGA, the results of the evaluation indicate that the model performs accurately, taking into account that current chemistry-transport model simulations underestimate the PM10 concentrations by 30–50%, using the current knowledge about aerosol physics and chemistry (Vautard et al., 2005). The slight underestimation in the NWM is produced since the emission model does not consider the re-suspension from soils and paved roads in urban areas (Lenschow et al., 2001; Viana et al., 2005), which may exert a limited influence in the PM10 levels in the area especially during the peak traffic hours.

A summary of the evaluation results is observed in the Table 5. The underestimation (mainly in the case of primary pollutants) is caused because the average volume defined by the model horizontal grid spacing must be sufficiently small to allow the air quality to be reproduced accurately, especially on

Table 5 – Summary of the average evaluation results in the air quality stations of the NWM

Statistic	O$_3$ ($\mu g\ m^{-3}$) NWM	BGA	NO$_2$ ($\mu g\ m^{-3}$) NWM	BGA	CO (mg m^{-3}) NWM	BGA	PM10 ($\mu g\ m^{-3}$) NWM	BGA
MB	2.151	−4.500	1.907	6.145	−0.109	−0.009	−8.217	−3.889
MNBE (%)	7.35%	−7.16%	6.24%	19.17%	−20.53%	−1.67%	−18.59%	−7.19%
MFB (%)	3.59%	−12.43%	1.16%	14.81%	−25.74%	−2.00%	−22.11%	−7.79%
MAGE	7.591	7.833	7.487	8.712	0.109	0.040	8.386	4.556
MNGE (%)	20.96%	25.81%	24.87%	24.47%	20.53%	7.84%	19.18%	9.55%
NME (%)	17.49%	23.98%	22.41%	20.06%	21.93%	8.04%	20.14%	9.81%
NMB (%)	4.96%	−13.78%	5.71%	14.15%	−21.93%	−1.87%	−19.74%	−8.37%
RMSE	9.755	9.327	9.567	10.881	0.155	0.046	10.704	5.175
UPA (%)	11.40%	−17.39%	−8.96%	−8.96%	−11.11%	−11.11%	−8.77%	−7.14%
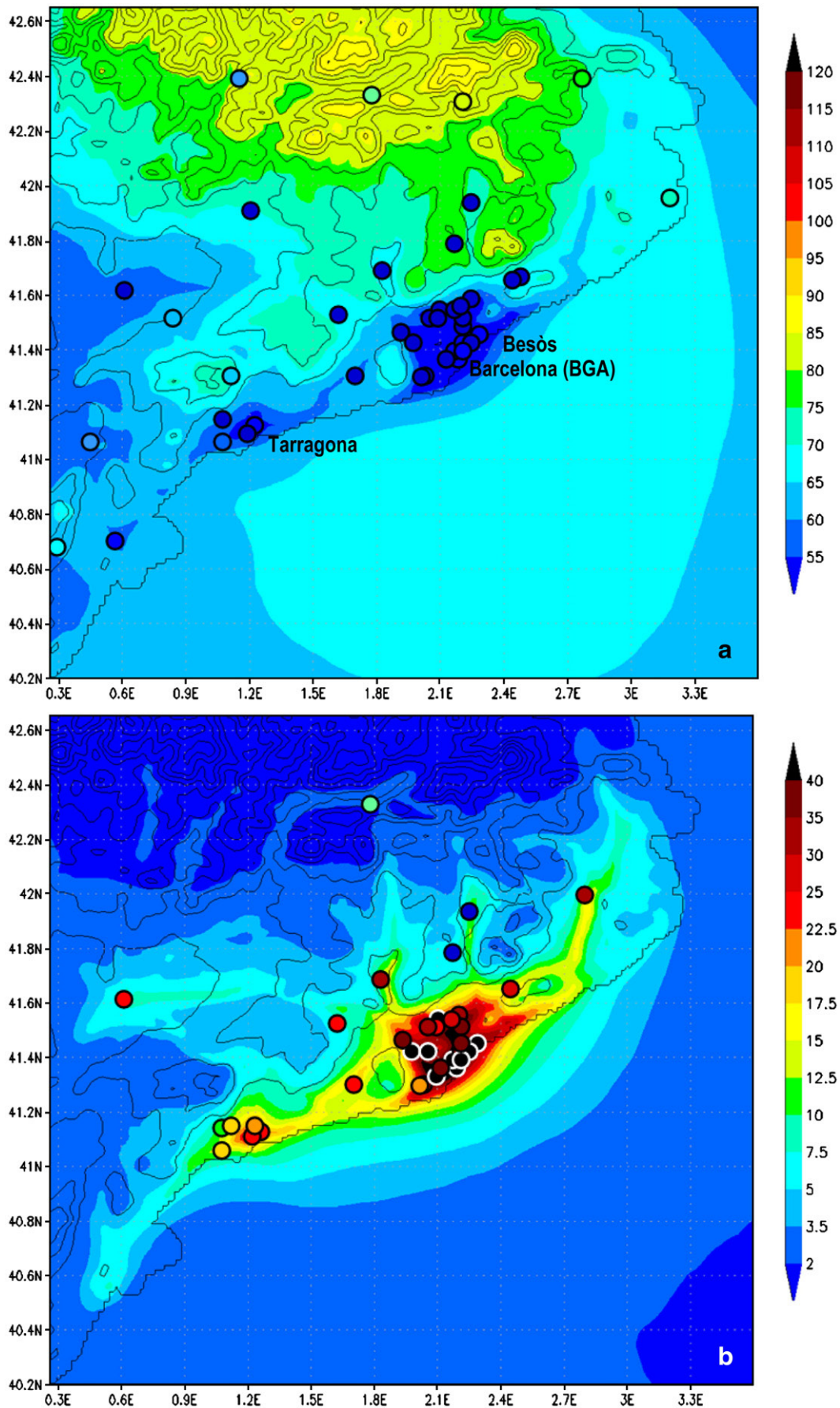
Fig. 3 – Evaluation of the model results (2-km resolution) vs. measurement data for annual model concentrations of the year 2004 (circles): (a) ozone, $\mu g\ m^{-3}$; (b) nitrogen dioxide, $\mu g\ m^{-3}$; (c) carbon monoxide, $mg\ m^{-3}$; and (d) particulate matter PM10, $\mu g\ m^{-3}$.
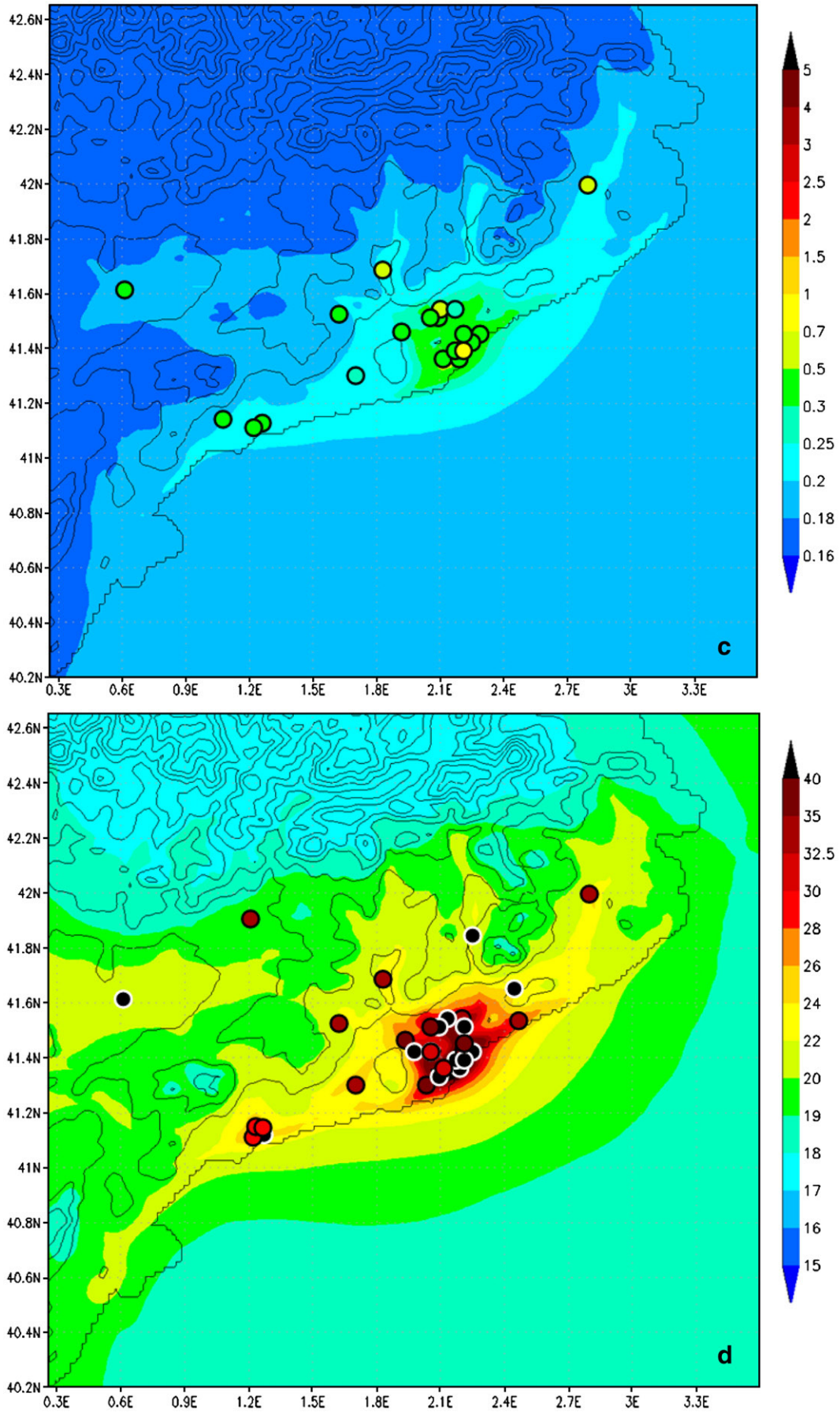
Fig. 3 (*continued*).
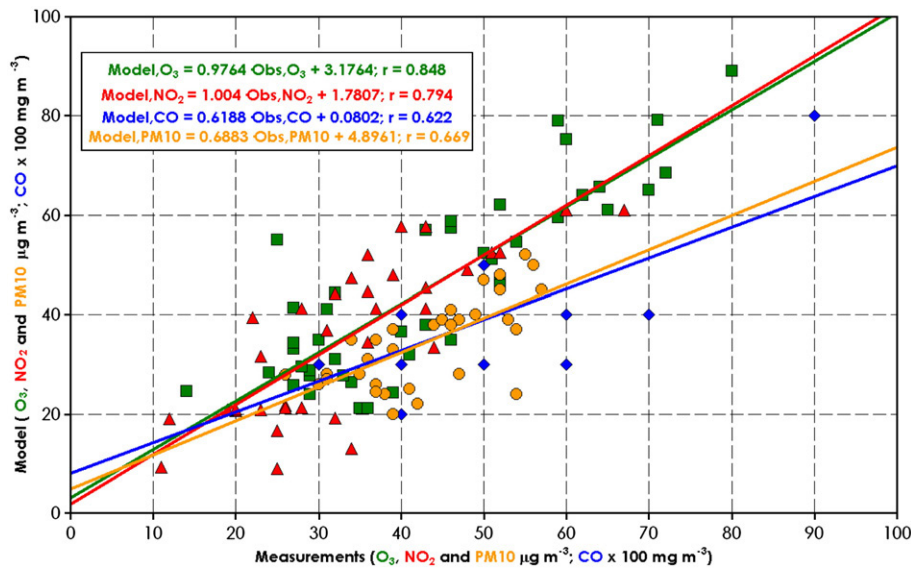
Fig. 4 – Correlation coefficients for model results versus observations: ozone (squares-green, μg m^{-3}); nitrogen oxides (triangles-red, μg m^{-3}); carbon monoxide (diamonds, blue, 100×mg m^{-3}); and particulate matter PM10 (orange-circles, μg m^{-3}).

urban scales (Jang et al., 1995). It appears that a finer grid is important for addressing air pollution processes in urban and industrial areas, whereas for rural areas larger grids may be allowed, for example, to capture the non-linearity of the ozone chemical formation as a function of precursor concentrations.

If the results of the evaluation are compared to the skill scores of previous works for several European models under the framework of the CityDelta project (e.g. Cuvelier et al., 2007; Thunis et al., 2007; Vautard et al., 2007; among others), the WRF/EMICAT/CMAQ/DREAM modelling system exhibits consistent scores for ozone (with mean values generally close to the observations–errors in the order of 20%) and a correlation coefficient of 0.848 (Cuvelier et al., 2007 report that most models show a r ranging from 0.4 and 0.8). Regarding the NO$_2$, high resolution applied in the area of study improves the results from previous studies (–80%); the errors obtained for the NWM are in the order of 25%. Also, the NO$_2$ correlation coefficient is 0.794 vs. 0.2–0.6 for CityDelta results. Last, for PM10, the results fully agree with previous works (biases of –20 to –50% vs.–19% for this work; correlation coefficient ranging from 0.4 to 0.75 vs. 0.669 in the case of applying WRF/EMICAT/CMAQ/DREAM in the NWMB).

3.3.   Annual air quality simulation

This section summarizes the results of the air quality simulations in the NWM for a 2-km resolution. The outputs of the model are compared with the values set in the legislation and analyses the exceedances of the thresholds set in the European regulations.

The Fig. 5a represents the annual 1-hr maximum O$_3$ concentration for the entire NWM during the annual cycle corresponding to the year 2004. The orange-dark red areas exceed the 180 μg m^{-3} set as the threshold for information to population set in the regulations. The areas with significant problems related to O$_3$ are the areas downwind the BGA. These

exceedances are caused by the transport of precursors from the BGA; the air masses act as photochemical reactors favouring the formation of O$_3$ from their precursors. Values over the information threshold are also reported by the model in BGA (harbour area) and Tarragona industrial area in the southern coast. The number of exceedances according to the simulations (not shown) is 14 h per year inland, downwind the BGA, meanwhile in the upwind area (Barcelona harbour area), the number of exceedances is 8 h per year. With respect to the annual average (Fig. 3a), the maximum concentration in the NWM is 95 μg m^{-3}. The highest values are diagnosed in the Pyrenees (around 90 μg m^{-3}), meanwhile the lowest values correspond to downtown Barcelona (under 30 μg m^{-3}).

For NO$_2$, the annual simulations present a 1-hr maximum (Fig. 5b) in the BGA (in the zone where the power generation facilities are located, named Besòs) of 233 μg m^{-3}. Therefore, this area exceeds the value for the protection of human health set in the Directive 1999/30/EC (200 μg m^{-3}, 1-hr average). Other areas with elevated concentrations are different locations in the BGA (with annual 1-hr maximum over 150 μg m^{-3}), the industrial area of Tarragona (150 μg m^{-3}) and the axis of the roads parallel to the coastline (1-hr maximum over 100 μg m^{-3}). For the annual average, the aforementioned Directive establishes the threshold for the protection of human health in 40 μg m^{-3}. Under this framework, the Fig. 3b indicates that this value is exceeded downtown Barcelona and in the Besòs industrial area (north-eastern part of the city of Barcelona). The rest of the BGA presents values ranging from 35 to 40 μg m^{-3}. The rest of areas in the NWM meet the reference values. In the urban areas, the elevated values are a consequence of the regional and urban background values and the direct emissions of traffic and other sources (Palmgren et al., 1999); however, the contribution of traffic to the exceedances of the thresholds may be over 80% (Crabbe et al., 1999).

In the case of carbon monoxide, the 1-hr maximum concentration during the year 2004 is 2.3 mg m^{-3} in the
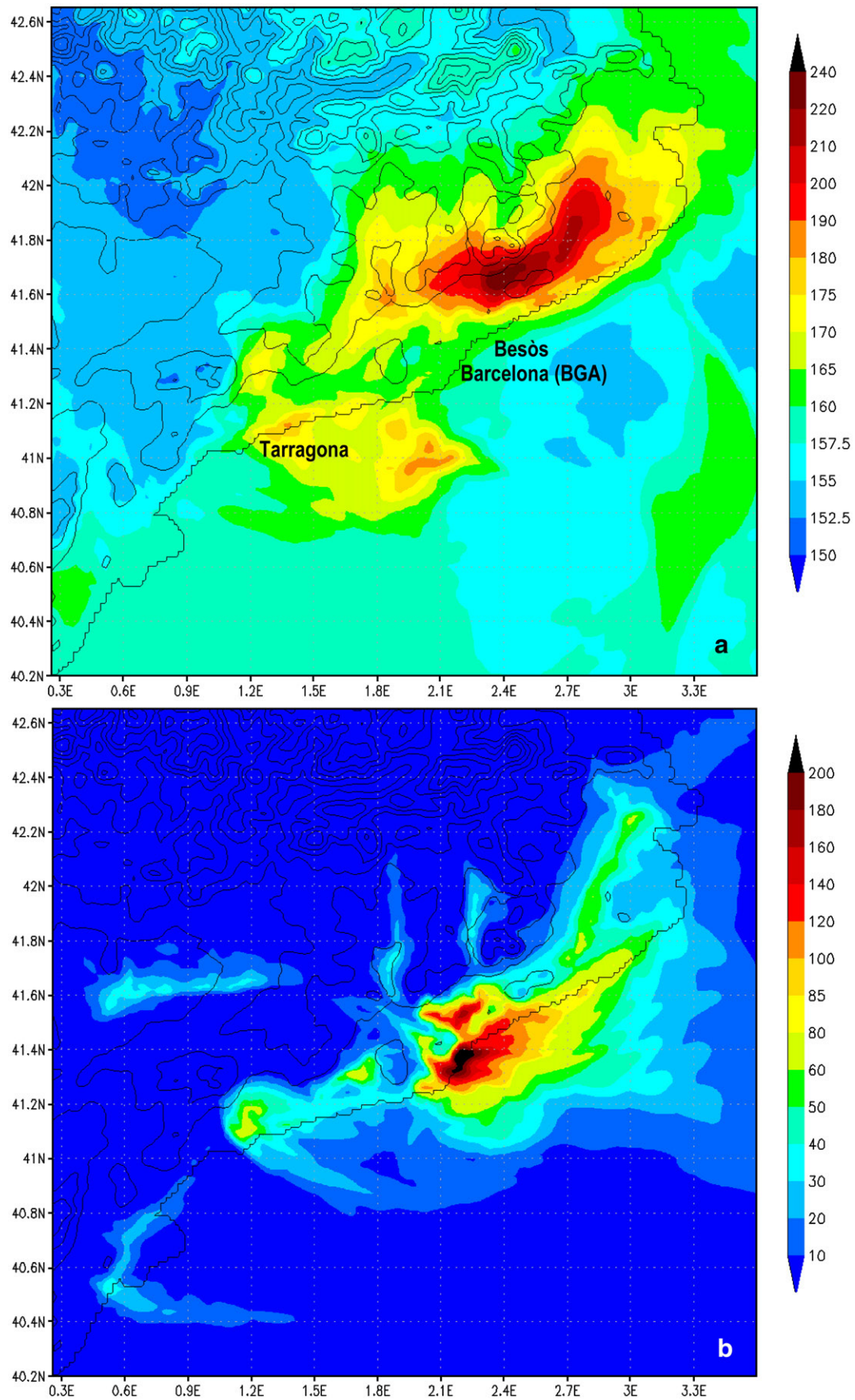
Fig. 5 – Annual 1-hr maximum concentration for the simulations (2-km resolution) for the year 2004: (a) ozone, $\mu g \, m^{-3}$; (b) nitrogen dioxide, $\mu g \, m^{-3}$; (c) carbon monoxide, $mg \, m^{-3}$; and (d) particulate matter PM10, $\mu g \, m^{-3}$.
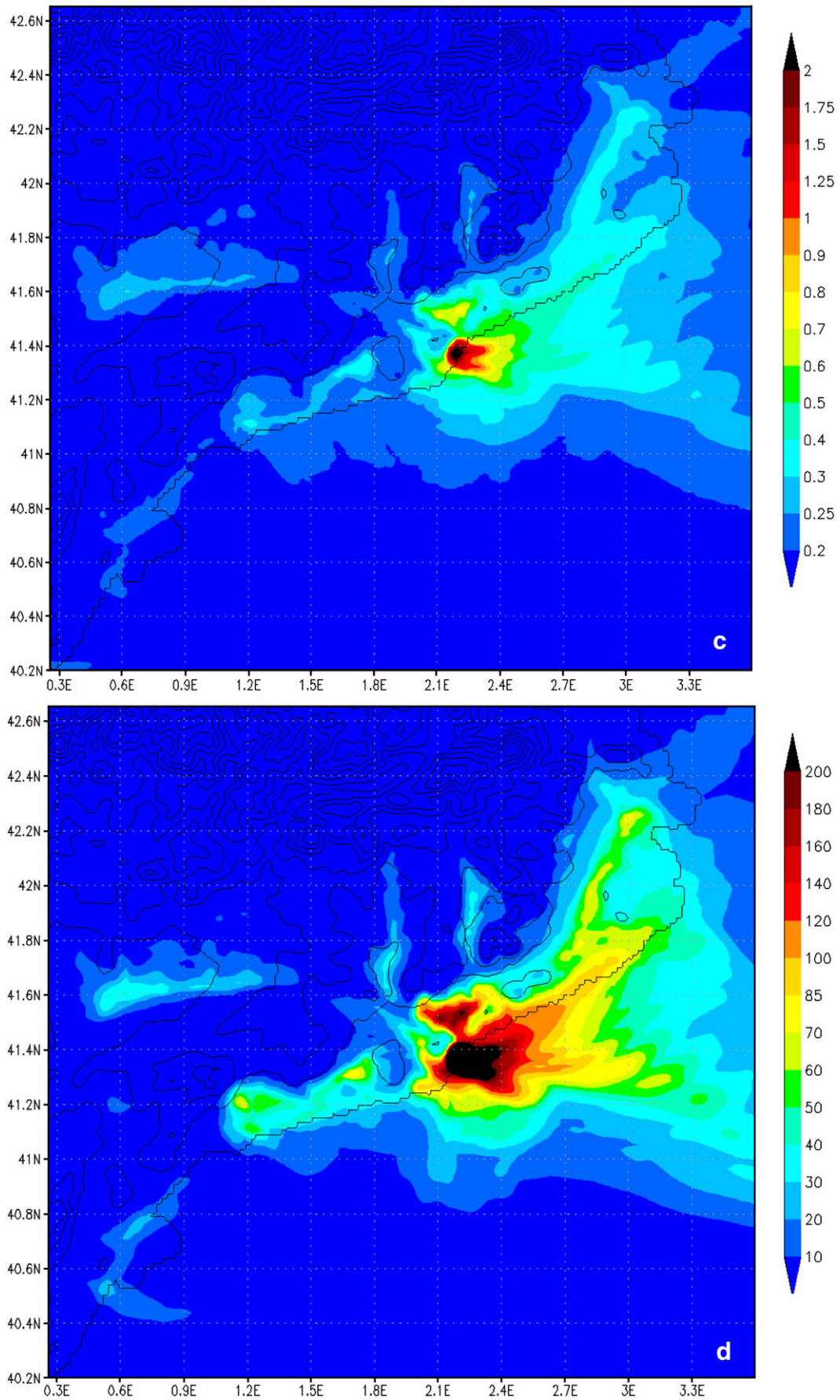
Fig. 5 (*continued*).

downtown area of the city of Barcelona (Fig. 5c), meanwhile the rest of the areas present values below 1.0 mg m^{-3}. The maximum annual average (Fig. 3c) is 0.32 mg m^{-3} in this same area, below the 10 mg m^{-3} established as the value for the protection of human health. Therefore, no problems related with carbon monoxide are observed in the NWM.

Mediavilla-Sahagún and ApSimon (2003) associate the most important health-related problems in urban areas with the exceedances of particulate matter. In the case of the PM10 in the NWM (taking into account the mineral dust, that is, considering both the anthropogenic and natural contribution), the modelling results indicate a 1-hr maximum concentration of 228 µg m^{-3} downtown Barcelona (Fig. 5d) and very high concentrations in all the BGA (ranging from 160 to 215 µg m^{-3} in the metropolitan area of Barcelona). Elevated 1-hr maximum values are also observed downwind the industrial area of Tarragona (southern coast) and the coastal highways of the NWM (up to 100 µg m^{-3}). For the 1-hr maximum values, there is no reference framework set in the legislation. The PM10 annual average (Fig. 3d) diagnosed in the BGA exceeds 50 µg m^{-3}, value set in the legislation for the protection of human health. We should bear in mind that these values (and also for the annual average) have been calculated with anthropogenic emissions (primary particulate matter and precursors of secondary aerosols), vegetation emissions (precursors of biogenic secondary organic aerosols) and the annual average contribution of mineral dust estimated by the DREAM model simulations, considered to be 4.9 µg m^{-3}. This is a key factor, since of the important contributions of Sahara/Sahel dust outbreaks in the Iberian Peninsula (Artíñano et al., 2001, Querol et al., 2001, 2004; Rodríguez et al., 2001; Viana et al., 2005; Pérez et al., 2006a,b).

4.   Conclusions

The application of state-of-the-art air quality models with high spatial and temporal resolution involves a novel approach in the NWM and the Iberian Peninsula. Up to date there are no studies of photochemical pollution that cover the NWM with a very high resolution on an annual basis that may contribute to the diagnosis of the state of air quality problems under a regulatory and decision-making perspective, because of the huge computational resources needed for a high-resolution annual regional simulation. The resolution applied requires of a great capacity of supercomputation, which is available with the MareNostrum supercomputer.

The simulations have been performed for the year 2004 with high spatial and temporal resolution (2 km and 1 h) in the NWM. The annual simulations come conditioned by the need for covering the different meteorological situations and types of episodes of air pollution in the area of study. At the same time, the 1-year numerical modelling allows comparing the values obtained with the reference values set in the regulations.

The outputs of the modelling system are compared with observations from 52 meteorological and 59 air quality stations belonging to the Environmental Department of the Catalonia Government (Spain), which involves a dense and accurate spatial distribution of stations in the territory (especially considering that they are distributed in an area of just 32,215 km^2). The results indicate a good behaviour of the model in both coastal and inland areas of the NWM, with a trend to the overestimation of tropospheric ozone concentrations and the underestimation of other photochemical pollutants (nitrogen dioxide, carbon monoxide and particulate matter).

In the case of ozone, the information threshold set in the Directive 2002/3/EC (180 µg m^{-3}) is exceeded in the area downwind the BGA. These exceedances are caused by the transport of pollutants from the city of Barcelona. Furthermore, punctual exceedances of the information thresholds are found in the industrial areas (mainly, the Barcelona port and the industrial area of Tarragona). For the nitrogen dioxide, the value for the protection of the human health (200 µg m^{-3} on an hourly basis and 40 µg m^{-3} for annual average) is diagnosed in Barcelona (especially at Besòs, in the north-eastern part of the city of Barcelona where powerplants are located). The concentrations of carbon monoxide are far below the 10 mg m^{-3} set in the regulations for the entire area of the NWM. Last, the 1-hr maximum concentration of PM10 simulated presents values frequently exceeding 100 µg m^{-3} in coastal areas and 200 µg m^{-3} in the BGA. With regards to annual value for the protection of human health (40 µg m^{-3}), it is exceeded in most of the BGA but not in the rest of the NWM. It should be highlighted that the particulate matter should include in future works the contribution of re-suspension from different paved roads for an accurate estimation of PM10 mainly in urban areas.

REFERENCES

Akimoto H. Global air quality and pollution. Science 2003;302:1716–9.
Ansmann A, Bösenber J, Chaikovsky A, Comerón A, Eckhardt S, Eixmann R, et al. Long-range transport of Saharan dust to northern Europe: the 11–16 October 2001 outbreak observed with EARLINET. J Geophys Res 2003;108(D24):4783. doi:10.1029/2003JD003757.
Artíñano B, Querol X, Salvador P, Rodríguez S, Alastuey A. Assessment of airborne particulate matter in Spain in response to the new EU-directive. Atmos Environ 2001;35:43–53.
Baldasano JM, Valera E, Jiménez P. Air quality data from large cities. Sci Total Environ 2003;307:141–65.

Balis D, Amiridis V, Kazadzis S, Papayannis A, Tsaknakis G, Tzortzakis S, et al. Optical characteristics of desert dust over the East Mediterranean during summer: a case study. Ann Geophys 2006;24:807–21.

Bougeault P, Jansá-Clar A, Benech B, Carissimo B, Pelon J, Richard E. Momentum budget over the Pyrenees: the PYREX experiment. Bull Am Meteorol Soc 1990;71:806–18.

Bougeault P, Benech P, Bessemoulin P, Carissimo B, Jansa-Clar A, Pelon J, et al. PYREX: a summary of findings. Bull Am Meteorol Soc 1997;78:637–50.

Byun DW, Ching JKS, editors. Science algorithms of the EPA Models-3 Community Multiscale Air Quality (CMAQ) Modelling System. EPA Report N. EPA-600/R-99/030, Office of Research and Development. Washington, DC: U.S. Environmental Protection Agency; 1999.

Coll I, Pinceloup S, Perros PE, Laverdet G, Le Bras G. 3D analysis of high ozone production rates observed during the ESCOMPTE campaign. Atmos Res 2005;74:477–505.

Cousin F, Tulet P, Rosset R. Interaction between local and regional pollution during ESCOMPTE 2001: impact on surface ozone concentrations (IOP2a and 2b). Atmos Res 2005;74:117–37.

Crabbe H, Beaumont R, Norton D. Local air quality management: a practical approach to air quality assessment and emissions audit. Sci Total Environ 1999;235:383–5.

Cros B, Durand P, Cachier H, Drobinski P, Fréjafon E, Kottmeier C, et al. The ESCOMPTE program: an overview. Atmos Res 2004;69:241–79.

Cuvelier C, Thunis P, Vautard R, Amann M, Bessagnet B, Bedogni M, et al. CityDelta: a model intercomparison study to explore the impact of emission reductions in European cities in 2010. Atmos Environ 2007;41:189–207.

Deng A, Seaman NL, Hunter GK, Stauffer DR. Evaluation of Interregional Transport using the MM5 SCIPUFF system. J Appl Metalwork 2004;43:1864–86.

Dueñas C, Fernández MC, Cañete S, Carretero J, Liger E. Assessment of ozone variations and meteorological effects in an urban area in the Mediterranean coast. Sci Total Environ 2002;299:97–113.

Dufour A, Amodei M, Ancellet G, Peuch VH. Observed and modelled chemical weather during ESCOMPTE. Atmos Res 2005;74:161–89.

EEA. Environment and Health. European Environment Agency, European Comission, Joint Research Centre, Report 10/2005, 2005; 40 pp.

Fast JD. Mesoscale modeling and four-dimensional data assimilation in areas of highly complex terrain. J Appl Met 1995;34:2762–82.

Fenger J. Urban air quality. Atmos Environ 1999;33:4877–900.

Gery MW, Whitten GZ, Killus JP, Dodge MC. A photochemical kinetics mechanism for urban and regional scale computer modelling. J Geophys Res 1989;94(D10):12925–56.

Gómez O, Baldasano JM. Biogenic VOC emission inventory for Catalonia, Spain. Proceedings of Eurotrac Symposium, vol. 2. 109:115.

Jang CJ, Jeffries HE, Byun D, Pleim JE. Sensitivity of ozone to model grid resolution — II. Detailed process analysis for ozone chemistry. Atmos Environ 1995;29(21):3101–14.

Jiménez P, Baldasano JM. Ozone response to precursor controls in very complex terrains: use of photochemical indicators to assess O_3–NO_x–VOC sensitivity in the north-eastern Iberian Peninsula. J Geophys Res 2004;109:D20309. doi:10.1029/2004JD004985.

Jiménez P, Dabdub D, Baldasano JM. Comparison of photochemical mechanisms for air quality modelling. Atmos Environ 2003;37:4179–94.

Jiménez P, Jorba O, Parra R, Baldasano JM. Influence of high-model grid resolution on photochemical modelling in very complex terrains. Int J Environ Pollut 2005a;24(1/2/3/4):180–200.

Jiménez P, Parra R, Baldasano JM. Modelling the ozone weekend effect in very complex terrains: a case study in the north-eastern Iberian Peninsula. Atmos Environ 2005b;39:429–44.

Jiménez P, Jorba O, Parra R, Baldasano JM. Evaluation of MM5-EMICAT2000-CMAQ performance and sensitivity in complex terrain: High-resolution application to the north-eastern Iberian Peninsula. Atmos Environ 2006a;40(26):5056–72. doi:10.1016/j.atmosenv.2005.12.060.

Jiménez P, Lelieveld J, Baldasano JM. Multiscale modelling of air pollutants dynamics in the north-western Mediterranean basin during a typical summertime episode. J Geophys Res 2006b;111:D18306. doi:10.1029/2005JD006516.

Jorba O, Gassó S, Baldasano JM. Regional circulations within the Iberian Peninsula east coast. In: Kluwer Academic/Plenum Publishers, editor. 26th Int. Tech. Meeting of NATO-CCMS on Air Pollution Modelling and its application; 2003. p. 388–95. Istanbul, Turkey, 26–30 May.

Kallos G. Regional/mesoscale models. In: Fenger J, Hertel O, Palmgren F, editors. Urban Air Pollution, European Aspects. Dordrecht: Kluwer Academic Publishers; 1998. p. 177–96.

Kalthoff N, Kottmeier C, Thürauf J, Corsmeier U, Saïd F, Frejafon E, et al. Mesoscale circulation systems and ozone concentrations during ESCOMPTE: a case study from IOP2b. Atmos Res 2005;74:355–80.

Lelieveld J, Berresheim H, Borrmann S, Crutzen PJ, Dentener FJ, Fischer H, et al. Global air pollution crossroads over the Mediterranean. Science 2002;298:794–9.

Lenschow P, Abraham HJ, Kutzner K, Lutz M, Preu JD, Reinchenbacher W. Some ideas about the sources of PM10. Atmos Environ 2001;35:23–33.

Lyons WA, Pielke RA, Tremback CJ, Walko RL, Moon DA, Keen CS. Modeling the impacts of mesoscale vertical motions upon coastal zone air pollution dispersion. Atmos Environ 1995;29:283–301.

Mediavilla-Sahagún A, ApSimon H. Urban scale integrated assessment of options to reduce PM10 in London towards attainment of air quality objectives. Atmos Environ 2003;37:4651–65.

Michalakes J, Dudhia J, Gill D, Henderson T, Klemp J, Skamarock W, et al. The weather research and forecast model: software architecture and performance. In: Zwieflhofer Walter, Mozdzynski George, editors. Proceedings of the Eleventh ECMWF Workshop on the Use of High Performance Computing in Meteorology. World Scientific; 2005. p. 156–68.

Millán MM, Artiñano B, Alonso L, Castro M, Fernandez-Patier R, Goberna J. Mesometeorological cycles of air pollution in the Iberian Peninsula. Air Pollution Research Report 44. Brussels, Belgium: Commission of the European Communities; 1992. 219 pp.

Millán MM, Salvador R, Mantilla E. Photooxidant dynamics in the mediterranean basin in summer. results from european research projects. J Geophys Res 1997;102(D7):8811–23.

Nickovic S, Papadopoulos A, Kakaliagou O, Kallos G. Model for prediction of desert dust cycle in the atmosphere. J Geophys Res 2001;106:18113–29.

Ntziachristos L, Samaras Z. COPERTIII Computer programme to calculate emissions from road transport. Methodology and emission factors (Version 2.1). Technical Report, vol. 49. European Environment Agency; 2000.

Palacios M, Kirchner F, Martilli A, Clappier A, Martín F, Rodríguez ME. Summer ozone episodes in the Greater Madrid area: analysis of the ozone response to abatement strategies by modelling. Atmos Environ 2002;36:5323–33.

Palacios M, Martín F, Aceña B. Estimate of potentially high ozone concentration areas in the centre of the Iberian Peninsula. Int J Environ Pollut 2004;24(1/2/3/4):260–71.

Palmgren F, Berkowicz R, Ziv A, Hertel O. Actual car fleet emissions estimated from urban air quality measurements and street pollution models. Sci Total Environ 1999;235:101–9.

Papayannis A, Zhang HQ, Amiridis V, Ju HB, Chourdakis G, Georgoussis G, et al. Extraordinary dust event over Beijing, China, during April 2006: Lidar, Sun photometric, satellite observations

and model validation. Geophys Res Lett 2007;34:L07806. doi:10.1029/2006GL029125.

Parra R, Jiménez P, Baldasano JM. Development of the high spatial resolution EMICAT2000 emission model for air pollutants from the north-eastern Iberian Peninsula of Catalonia, Spain. Environ Pollut 2006;140(2):200–19. doi:10.1016/j.envpol.2005.07.021.

Pérez C, Sicard M, Jorba O, Comerón A, Baldasano JM. Summertime re-circulations of air pollutants over the north-eastern Iberian coast observed from systematic EARLINET lidar measurements in Barcelona. Atmos Environ 2004;38:3983–4000.

Pérez C, Nickovic S, Pejanovic G, Baldasano JM, Özsoy E. Interactive dust-radiation modelling: a step to improve weather forecast. J Geophys Res 2006a;111:D16206. doi:10.1029/2005JD006717.

Pérez C, Nickovic S, Baldasano JM, Sicard M, Rocadenbosh F, Cachorro VE. A long Saharan dust event over the western Mediterranean: Lidar, sun photometer observations and regional dust modelling. J Geophys Res 2006b;111:D15214. doi:10.1029/2005JD006579.

Pleim JE, Clarke JF, Finkelstein PL, Cooter EJ, Ellestad TG, Xiu A, et al. Comparison of measured and modelled surface fluxes of heat, moisture and chemical dry deposition. In: Schiermeier Gryning, editor. Air Pollution Modeling and its Application XI. New York: Plenum Press; 1996.

Querol X, Alastuey A, Podríguez S, Plana F, Ruiz CR, Cots N, et al. PM10 and PM2.5 source apportionment in the Barcelona Metropolitan Area, Catalonia, Spain. Atmos Environ 2001;35(36):6407–19.

Querol X, Alastuey A, Rodríguez S, Viana M, Artiñano B, Salvador P, et al. Levels of particulate matter in rural, urban and industrial sites in Spain. Sci Total Environ 2004;334–335:359–76.

Reis S, Simpson D, Friedrich R, Jonson JE, Unger S, Obermeier A. Road traffic emissions predictions of future contributions to regional ozone levels in Europe. Atmos Environ 2000;34:4701–10.

Ribas A, Peñuelas J. Temporal patterns of surface ozone levels in different habitats of the North Western Mediterranean basin. Atmos Environ 2004;38:985–92.

Rodríguez S, Querol X, Alastuey A, Kallos G, Kakaliagou O. Saharan dust contribution to PM10 and TSP levels in Southern and Eastern Spain. Atmos Environ 2001;35:2433–47.

Rodríguez S, Querol X, Alastuey A, Plana F. Sources and processes affecting levels and composition of atmospheric aerosol in the Western Mediterranean. J Geophys Res 2002;107(D24):4777.

Russell A, Dennis R. NARSTO critical review of photochemical models and modelling. Atmos Environ 2000;34:2283–324.

Sanz MJ, Millán M. The dynamics of polluted airmases and ozone cycles in the western Mediterranean: relevance to forest ecosystems. Chemosphere 1998;98(36):1089–94.

Sanz MJ, Calatayud V, Calvo E. Spatial pattern of ozone injury in Aleppo pine related to air pollution dynamics in a coastal-mountain region of eastern Spain. Environ Pollut 2000;108:239–47.

Seaman NL, Stauffer DR, Lario-Gibbs AM. A multiscale four dimensional data assimilation system applied in the San Joaquin valley during SARMAP. Part I: Modeling design and basic performance. J Appl Metalwork 1995;34:1739–61.

Seinfeld JH. Ozone air quality models: a critical review. JAPCA 1988;38(5):616–45.

Shafran PC, Seaman NL, Gayno GA. Evaluation of numerical predictions of boundary layer structure during the Lake-Michigan Ozone Study (LMOS). J Appl Metalwork 2000;39:412–26.

Sicard M, Pérez C, Rocadenbosch F, Baldasano JM, García-Vizcaino D. Mixed layer depth determination in the Barcelona costal area from regular lidar measurements: methods, results and limitations. Bound-Lay Met 2006;119:135–57.

Skamarock WC, Klemp JB, Dudhia J, Gill DO, Barker DM, Wang W, et al. A description of the Advanced Research WRF Version 2. NCAR Tech Notes-468+STR; 2005.

Streit GE, Guzmán F. Mexico City air quality: progress on an international collaborative project to define air quality management options. Atmos Environ 1996;30(5):723–33.

Thunis P, Rouil L, Cuvelier C, Stern R, Kerschbaumer A, Bessagnet B, et al. Analysis of model responses to emission-reduction scenarios within the CityDelta project. Atmos Environ 2007;31:208–20.

Ulrickson BL, Mass CF. Numerical investigation of mesoscale circulations in the Los Angeles basin. Part I: A verification study. Mon Weather Rev 1990;118:2138–61.

US EPA. Guideline for Regulatory Application of the Urban Airshed Model. US EPA Report No. EPA-450/4-91-013. Office of Air and Radiation, Office of Air Quality Planning and Standards, Technical Support Division. North Carolina, US: Research Triangle Park; 1991.

US EPA. Guidance on the use of models and other analyses in attainment demonstrations for the 8-hour ozone NAAQS. US EPA Report No. EPA-454/R-05-002. Office of Air Quality Planning and Standards. North Carolina, US: Research Triangle Park; 2005. October 2005, 128 pp.

Vautard R, Bessagnet B, Chin M, Menut L. On the contribution of natural Aeolian sources to particulate matter concentrations in Europe: testing hypotheses with a modelling approach. Atmos Environ 2005;39:3291–303.

Vautard R, Builtjes PHJ, Thunis P, Cuvelier C, Bedogni M, Bessagnet B, et al. Evaluation and intercomparison of Ozone and PM10 simulations by several chemistry transport models over four European cities within the CityDelta project. Atmos Environ 2007;41:173–88.

Viana M, Pérez C, Querol X, Alastuey A, Nickovic S, Baldasano JM. Spatial and temporal variability of PM levels and composition in a complex summer atmospheric scenario in Barcelona (NE Spain). Atmos Environ 2005;39:5343–61.

Vinuesa JF, Mirabel P, Ponche JL. Air quality effects of using reformulated and oxygenated gasoline fuel blends application to the Strasbourg area (F). Atmos Environ 2003;37:1757–74.

Wang Y, Jacob DJ, Logan JA. Global simulation of tropospheric O_3–NO_x-hydrocarbon chemistry, 2, Model evaluation and global ozone budget. J Geophys Res 1998;103:10727–55.

Whitemann CD. Mountain Meteorology. Fundamentals and Applications. New York-Oxford: Oxford University Press; 2000. 356 pp.

Ziomas IC, Gryning SE, Borstein RD. The Mediterranean campaign of photochemical tracers-transport and chemical evolution (MEDCAPHOT-TRACE). Atmos Environ 1998;32:2043–326.